

MR-blob: Coordinate-Transformed Blobs for Parallel MRI Reconstruction

Imraj RD Singh¹, Željko Kereta¹, Alexander Denker², Riccardo Barbano³,
Bangti Jin⁴, Kris Thielemans^{5,6}, and Simon Arridge¹

¹Department of Computer Science, University College London, United Kingdom

²Center of Industrial Mathematics (ZeTeM), University of Bremen, Germany

³School of Computation, Information and Technology, Technical University of Munich, Germany

⁴Department of Mathematics, The Chinese University of Hong Kong, Hong Kong

⁵Institute of Nuclear Medicine, University College London, United Kingdom

⁶Centre for Medical Imaging Computing, University College London, United Kingdom

SYNOPSIS

Motivation: Reducing the number of parameters needed to represent and reconstruct parallel MRI measurements. **Goal:** Reconstruct parallel MRI measurements with coordinate-transformed Gaussian functions (blobs) where the forward model is formulated directly. We term this MR-blob. **Approach:** MR-blob directly represents parallel MRI measurements; where coil sensitivities are modelled as isotropic Gaussians and the image is represented by coordinate-transformed blobs. **Results:** Noisy, undersampled parallel MRI simulations of Shepp-Logan phantom are reconstructed with a pixelised image, a coordinate-transformed blob-based image, and MR-blob; all with total variation regularisation. Quality measures are shown to be consistent across methods and regularisation strengths.

Keywords: parallel imaging, reconstruction, MRI, blobs

IMPACT

Parameter-efficient image representations have the potential to reduce computational burden. This work defines parallel MRI forward model for coordinate-transformed blobs. This includes auto-calibrating coil sensitivities that re-scale and translate to fit the parallel MRI measurements.

INTRODUCTION

Images are functions defined on two continuous spatial coordinates r_x and r_y , and are discretised to allow for digital processing. The most prevalent discretisation is via equally-spaced piece-wise-constant basis functions, aka pixels. Other local basis functions have been developed¹ and applied to image reconstruction.^{2,3} This work investigates the use of Gaussian functions, herein referred to as blobs. These blobs are locally defined, and to globally represent an image a set of blobs is typically fixed as an equally-spaced lattice of specific scale. Recently, Gaussian splats were proposed⁴ that parameterise and optimise the covariance of the blobs. This was shown to be effective and efficient for radiance field rendering. We re-parameterise Gaussian splats as coordinate-transformed blobs. Using such coordinate-transformed blobs, we develop a forward model to reconstruct parallel MRI measurements and auto-calibrate the coil sensitivities; this is termed as MR-blob.

COORDINATE-TRANSFORMED BLOBS

We consider coordinate transformed blobs of the form:

$$b(\mathbf{r}) = b(\mathbf{r}; c, \mathbf{T}, \mathbf{t}) = c \exp\left(-\frac{1}{2} \hat{\mathbf{r}}(\mathbf{r})^\top \hat{\mathbf{r}}(\mathbf{r})\right), \text{ for } \hat{\mathbf{r}}(\mathbf{r}) = \mathbf{T}\mathbf{r} + \mathbf{t} = \begin{bmatrix} \mathcal{S}^{x,x} & \mathcal{S}^{x,y} \\ \mathcal{S}^{y,x} & \mathcal{S}^{y,y} \end{bmatrix} \begin{bmatrix} r_x \\ r_y \end{bmatrix} + \begin{bmatrix} t_x \\ t_y \end{bmatrix}, \quad (1)$$

where $\mathbf{r} = [r_x, r_y]^\top$ is the coordinate system, and c the contrast. Herein \mathbf{T} is a general linear transform of the coordinate system, and \mathbf{t} is translation. A coordinate transformed blob can be rewritten as:

$$b(\mathbf{r}) = c\mathcal{N}(\mathbf{r}; -\mathbf{T}^{-1}\mathbf{t}, (\mathbf{T}^\top\mathbf{T})^{-1}), \quad (2)$$

where $\mathcal{N}(\mathbf{r}; \boldsymbol{\mu}, \boldsymbol{\Sigma}) = \exp(-\frac{1}{2}(\mathbf{x} - \boldsymbol{\mu})^\top \boldsymbol{\Sigma}^{-1}(\mathbf{x} - \boldsymbol{\mu}))$ is the un-normalised Gaussian function with mean $\boldsymbol{\mu}$ and covariance $\boldsymbol{\Sigma}$. To represent more complex functions, e.g., images, an ensemble of blobs is used:

$$B(\mathbf{r}) = B(\mathbf{r}; C, \Phi) := \sum_{i=1}^{N_b} b(\mathbf{r}; c_i, \mathbf{T}_i, \mathbf{t}_i). \quad (3)$$

We define $C = \{c_i\}_{i=1}^{N_b}$ as *contrast* and $\Phi = \{(\mathbf{T}_i, \mathbf{t}_i)\}_{i=1}^{N_b}$ as the *basis* of the coordinate-transformed blobs.

SINGLE COIL MODELLING

Coil sensitivities are modelled as un-normalised isotropic Gaussians:

$$b_\kappa(\mathbf{r}) = b_\kappa(\mathbf{r}; s_\kappa, \boldsymbol{\mu}_\kappa) := \mathcal{N}(\mathbf{r}; \boldsymbol{\mu}_\kappa, s_\kappa^2 \mathbf{I})$$

with scale s_κ and centre $\boldsymbol{\mu}_\kappa$. The coil sensitivity acts such that signal closer to the centre is stronger and decays in space exponentially. A coil image, the coil sensitivities on the image, is modelled as:⁵

$$b_\kappa(\mathbf{r}; s_\kappa, \boldsymbol{\mu}_\kappa) \cdot B(\mathbf{r}; C, \Phi) = \sum_{i=1}^{N_b} k_{\kappa,i} \mathcal{N}(\mathbf{r}; \boldsymbol{\mu}_{\kappa,i}, \boldsymbol{\Sigma}_{\kappa,i}),$$

where

$$\begin{aligned} \boldsymbol{\Sigma}_{\kappa,i} &= (\mathbf{T}_i^\top \mathbf{T}_i + s_\kappa^2 \mathbf{I}), \quad \boldsymbol{\mu}_{\kappa,i} = \boldsymbol{\Sigma}_{\kappa,i}^{-1} (-\mathbf{T}_i^\top \mathbf{t}_i + s_\kappa^2 \boldsymbol{\mu}_\kappa), \\ k_{\kappa,i} &= c_i \sqrt{\det(\boldsymbol{\Sigma}_{\kappa,i}^{-1})} \exp\left(-\frac{1}{2}(-\mathbf{T}_i^{-1}\mathbf{t}_i - \boldsymbol{\mu}_\kappa)^\top \boldsymbol{\Sigma}_{\kappa,i}^{-1}(-\mathbf{T}_i^{-1}\mathbf{t}_i - \boldsymbol{\mu}_\kappa)\right) \end{aligned} \quad (4)$$

MRI measurements acquired by a coil are in the frequency (k-space) domain. These can be modelled in k-space coordinates $\mathbf{k} = [k_x, k_y]^\top$ by Fourier transforming $b_\kappa(\mathbf{r}) \cdot B(\mathbf{r})$:

$$\mathcal{F}\{b_\kappa(\mathbf{r}; s_\kappa, \boldsymbol{\mu}_\kappa) \cdot B(\mathbf{r}; C, \Phi)\}(\mathbf{k}) = \mathcal{F}\{k_{\kappa,i} \mathcal{N}(\mathbf{r}; \boldsymbol{\mu}_{\kappa,i}, \boldsymbol{\Sigma}_{\kappa,i})\}(\mathbf{k}) \quad (5)$$

$$= \sum_{i=1}^{N_b} \frac{2\pi k_{\kappa,i}}{\sqrt{\det(\boldsymbol{\Sigma}_{\kappa,i})}} \exp\left(-i\mathbf{k}^\top \boldsymbol{\mu}_{\kappa,i} - \frac{1}{2}\mathbf{k}^\top \boldsymbol{\Sigma}_{\kappa,i} \mathbf{k}\right). \quad (6)$$

MR-BLOB: FORMULATION AND INVERSE PROBLEM

We define the MR-blob as:

$$\text{MR-blob}(\mathbf{k}; S, M, C, \Phi) := \begin{pmatrix} \mathcal{F}(b_1(\mathbf{r}; s_1, \boldsymbol{\mu}_1) \cdot B(\mathbf{r}; C, \Phi))(\mathbf{k}) \\ \vdots \\ \mathcal{F}(b_{N_\kappa}(\mathbf{r}; s_{N_\kappa}, \boldsymbol{\mu}_{N_\kappa}) \cdot B(\mathbf{r}; C, \Phi))(\mathbf{k}) \end{pmatrix}. \quad (7)$$

The parameters of the coils are scales $S := \{s_\kappa\}_{\kappa=1}^{N_\kappa}$ and centres $M := \{\boldsymbol{\mu}_\kappa\}_{\kappa=1}^{N_\kappa}$. The same contrast C and basis Φ are used across all coils. The inverse problem is given by:

$$\text{MR-blob}(\mathbf{k}; S, M, C, \Phi) = G(\mathbf{k}),$$

where parallel MRI measurements are $G: \Omega_k \mapsto \mathbb{C}^{N_\kappa}$ with $N_\kappa \in \mathbb{N}$ coils. The domain $\Omega_k = \{\mathbf{k}_n\}_{n=1}^{N_k}$ is a set of coordinates with $N_k \in \mathbb{N}$ measurements.

In the variational framework of inverse problems,⁶ we recover the parameters of the reconstruction through optimising:

$$S^*, M^*, C^*, \Phi^* \in \min_{S, M, C, \Phi} \left\{ \frac{1}{N_k} \sum_{n=1}^{N_k} \|\text{MR-blob}(\mathbf{k}_n; S, M, C, \Phi) - G(\mathbf{k}_n)\|^2 + \lambda R(B(\mathbf{r}; C, \Phi)) \right\}, \quad (8)$$

where the first term promotes data-consistency, and the second is a regulariser with strength λ . We directly optimise over blob parameters (contrast C and basis Φ), as well as over the coil sensitivities, specified by S and M . Thus, we jointly reconstruct the image and calibrate the coil sensitivities. The reconstruction $f : \Omega_r \mapsto \mathbb{C}$ with $\Omega_r = \{\mathbf{r}_m\}_{m=1}^{N_r}$ is given by

$$f(\mathbf{r}) = B(\mathbf{r}; C^*, \Phi^*). \quad (9)$$

We study two regularisers:

$$R_{\text{cond}}(\Phi) := \frac{1}{N_b} \sum_{i=1}^{N_b} \text{cond}(\mathbf{T}_i^\top \mathbf{T}_i), \quad (10)$$

$$R_{\text{TV}}(\Omega_r; C, \Phi) := \frac{1}{N_r} \sum_{m=1}^{N_r} R_{\text{TV}}(\mathbf{r}_m; C, \Phi), \quad \text{with } R_{\text{TV}}(\mathbf{r}; C, \Phi) := \|\nabla_{\mathbf{r}} B(\mathbf{r}; C, \Phi)\|_1, \quad (11)$$

promoting blob skewness and TV sparsity, respectively. We optimise Eqn. (8) by taking the gradients using automatic (reverse-mode) differentiation with the first-order ADAM optimiser.⁷

METHODS

Three methods were compared to illustrate the features of reconstruction with pixels (M1), blobs (M2) and MR-blobs (M3). We denote the pixelised image as $\mathbf{f} \in \mathbb{C}^{N_r}$, and Non-Uniform-Fast-Fourier-Transform (NUFFT) with coil sensitivities forward model as $\mathbf{A} : \mathbb{C}^{N_r} \mapsto \mathbb{C}^{N_k \times N_k}$. The corresponding objective functions are given by

$$\text{M1 (Pixels): } \min_{\mathbf{f}} \left\{ \frac{1}{N_k} \|\mathbf{A}\mathbf{f} - G(\Omega_k)\|_F^2 + \frac{\lambda}{N_r} \|\nabla \mathbf{f}\|_1 \right\} \quad (12)$$

$$\text{M2 (Blobs): } \min_{C, \Phi} \left\{ \frac{1}{N_k} \|\mathbf{A}B(\Omega_r; C, \Phi) - G(\Omega_k)\|_F^2 + 10 \cdot R_{\text{cond}}(\Phi) + \lambda R_{\text{TV}}(\Omega_r; C, \Phi) \right\} \quad (13)$$

$$\text{M3 (MR-blob): } \min_{S, M, C, \Phi} \left\{ \frac{1}{N_k} \sum_{n=1}^{N_k} \|\text{MR-blob}(\mathbf{k}_n; S, M, C, \Phi) - G(\mathbf{k}_n)\|^2 + 10 \cdot R_{\text{cond}}(\Phi) + \lambda R_{\text{TV}}(\Omega_r; C, \Phi) \right\}, \quad (14)$$

where $G(\Omega_k) := [G(\mathbf{k}_1), \dots, G(\mathbf{k}_{N_k})]$ and $B(\Omega_r; C, \Phi) := [B(\mathbf{r}_1; C, \Phi), \dots, B(\mathbf{r}_{N_r}; C, \Phi)]^\top$. TV regularisation of the same λ was tested for all three methods. For M2 and M3 we include a constant skew-penalisation and evaluate TV at points corresponding to pixel centres.

DISCUSSION AND CONCLUSION

The same forward model used for simulation is used for reconstruction for M1 and M2. With coil sensitivities of MR-blob initially centred in the image, the auto-calibration allows the coils to translate and re-scale to fit the measurements. This resulted in the coil sensitivities and coil images shown in Fig. 5. Further, the piece-wise-constant structure of the Shepp-Logan phantom is not well approximated by smooth basis functions such as blobs. Notwithstanding, it is observed that blob-based images give competitive performance with $2.6\times$ less parameters than pixels. Additionally, the smoothness of blobs provides implicit regularisation at lower regularisation values. The M2 and M3 reconstructions exhibit bases Φ with prominent structure, see Fig. 4. It is noted that M3 gave fewer zero contrasts, less skewed blobs and a larger range of scales compared to M2.

The data-consistency terms of M2 and M3 are smooth given positive-definite covariances, but highly non-convex. The optimisation could benefit from more specialised algorithm. This will be investigated further where acceleration would benefit from scaling to 3D in-vivo measurements. We have shown coordinate-transformed blobs are able to approximate parallel MRI reconstructions efficiently and accurately. Given the simplicity of the formulation it is amenable to rigorous analysis, and we leave that for future work.

Number of blobs	30^2
Blob parameters	6,300
Acceleration factor	$2.6 \times$
Initial spacing	Equispaced lattice
Initial shape	Constant isotropic
Initial c	Zeros

Phantom	128^2 Shepp Logan
k space trajectory	25 radial spokes
Spoke offset	Golden angle
Acceleration factor	$9.7 \times$
k space data SNR	20 dB
Number of coils	5

Quality Measure	Acronym	Note
Peak Signal to Noise Ratio	PSNR	Global image quality
Structural Similarity Index Measure	SSIM	Global image quality
Data Fidelity	DF	MSE k space domain
Contrast recovery coefficient	CRC	See below



A local image quality metric, higher values the better contrast recovery. CRC is computed between a ROI on the three small ellipses (red) and background (blue) of the figure on the right.

Figure 1. Top left: ensemble of coordinate blobs specification and initialisation. Top right: phantom and data simulation. Bottom: quality measures used in the study.

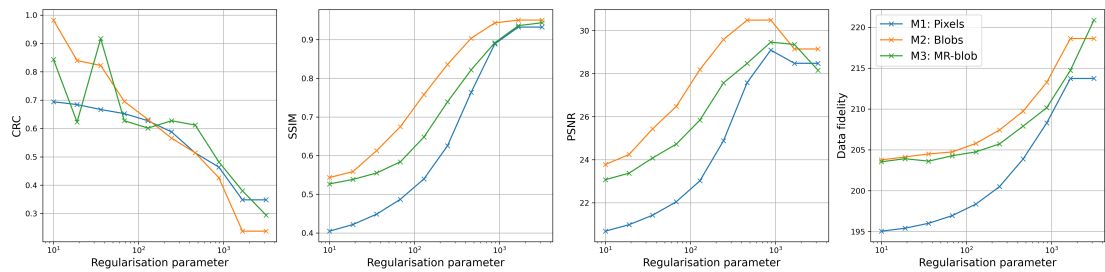


Figure 2. CRC, SSIM, PSNR, DF for all three methods swept over the same range of regularisation parameters ($\log_{10}(\lambda) \in \{1.00, 1.28, 1.56, 1.83, 2.11, 2.39, 2.67, 2.94, 3.22, 3.50\}$).

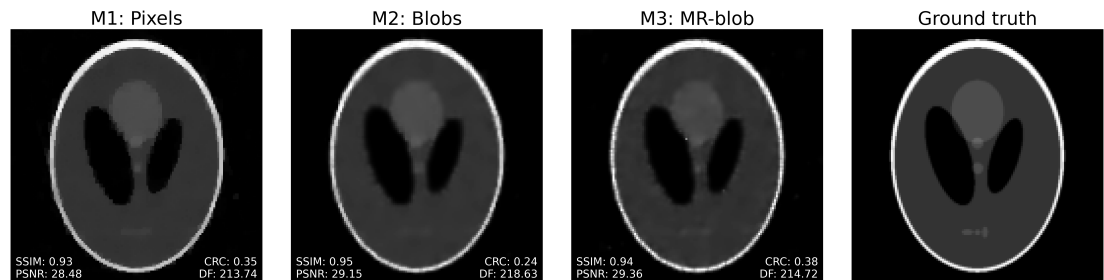


Figure 3. Well-regularised reconstructions ($\lambda = 1,668$) from noisy, under-sampled measurements. Note the instability exhibited in MR-blob reconstruction.

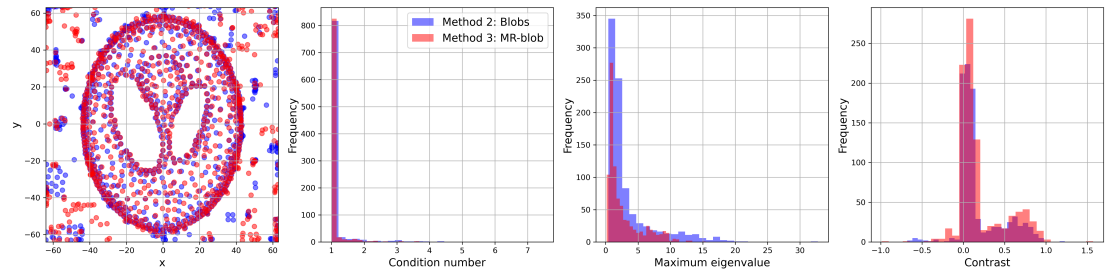


Figure 4. Coordinate transformed blob parameters of well-regularised ($\lambda = 1,668$) M2 and M3 reconstructions. Left: mean of blobs. Centre left: Condition number of covariance (skewness). Centre right: Maximum eigenvalue (scale) of covariance. Right: Contrast of blobs.

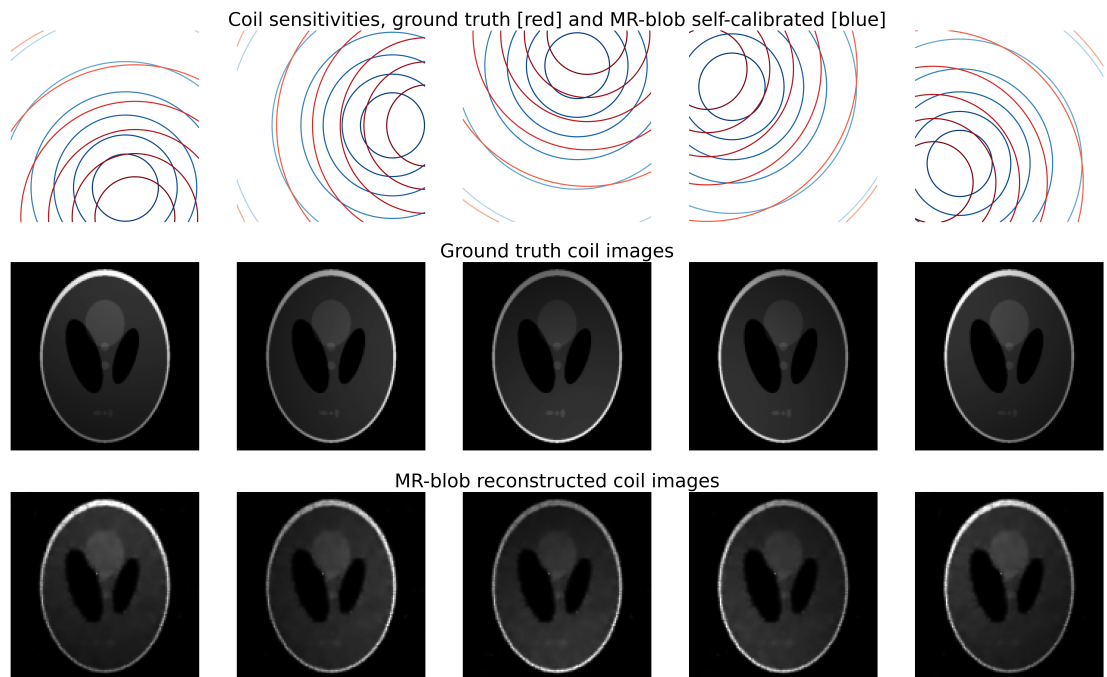


Figure 5. Top row: Ground truth (red) and MR-blob auto-calibrated (blue) coil sensitivities, MR-blob coils were initialised at the centre at set scale. Middle row: Ground truth coil images. Bottom row: Well-regularised ($\lambda = 1,668$) MR-blob reconstructed coil images. Columns correspond to individual coils.

ACKNOWLEDGMENTS

I.R.D. Singh was supported by the EPSRC-funded UCL Centre for Doctoral Training in Intelligent, Integrated Imaging in Healthcare (i4health) (EP/S021930/1) and the Department of Health's NIHR-funded Biomedical Research Centre at University College London Hospitals. Ž. Kereta was supported by the UK EPSRC grant EP/X010740/1. A. Denker was supported by the Deutsche Forschungsgemeinschaft (DFG, German Research Foundation) - Project number 281474342/GRK2224/2. B. Jin and S. Arridge were supported by the UK EPSRC EP/V026259/1. The authors would like to thank Mark Griswold and Pete Lally for their fruitful discussion.

REFERENCES

- ¹ Kenneth M Hanson and George W Wecksung. Local basis-function approach to computed tomography. *Applied Optics*, 24(23):4028–4039, 1985.
- ² Robert M Lewitt. Alternatives to voxels for image representation in iterative reconstruction algorithms. *Physics in Medicine & Biology*, 37(3):705, 1992.
- ³ Simon R Arridge and Martin Schweiger. Image reconstruction in optical tomography. *Philosophical Transactions of the Royal Society of London. Series B: Biological Sciences*, 352(1354):717–726, 1997.
- ⁴ Bernhard Kerbl, Georgios Kopanas, Thomas Leimkühler, and George Drettakis. 3d Gaussian splatting for real-time radiance field rendering. *ACM Transactions on Graphics (ToG)*, 42(4):1–14, 2023.
- ⁵ Kaare Brandt Petersen, Michael Syskind Pedersen, et al. The matrix cookbook. *Technical University of Denmark*, 7(15):510, 2008.
- ⁶ Otmar Scherzer, Markus Grasmair, Harald Grossauer, Markus Haltmeier, and Frank Lenzen. *Variational methods in imaging*, volume 167. Springer, 2009.
- ⁷ Diederik P Kingma and Jimmy Ba. Adam: A method for stochastic optimization. *arXiv preprint arXiv:1412.6980*, 2014.